Effect of eggshell powder calcined at different temperatures on the workability and mechanical properties of cement-based mortars

Farklı sıcaklıklarda kalsine edilmiş yumurta kabuğu tozunun çimento esaslı harçların işlenebilirlik ve mekanik özellikleri üzerindeki etkisi

Ahmet Ferdi Şenol[1], [iD], Özlem Çalışkan[2*] [iD]

[1,2] Bilecik Şeyh Edebali University, Faculty of Engineering, Civil Engineering Department, 11100, Bilecik, Türkiye

Abstract

In this study, the incorporation of waste eggshell powder (ESP), a calcium carbonate ($CaCO_3$)-rich by-product of the food industry, into cement-based mortars was investigated. Eggshells were ground and calcined at 800 °C and 900 °C for two hours to produce ESP800 and ESP900. ESP replaced cement at 5%, 10%, and 15% by weight, yielding seven mortar mixtures. Thermal and microstructural properties were examined by TG/DSC, FE-SEM, and XRD. Workability was assessed with the flow table test, and specimens cured for 7 and 28 days were tested for ultrasonic pulse velocity (UPV), flexural strength (FS), and compressive strength (CS). Calcination temperature and replacement level significantly influenced performance. At 5% replacement, ESP900-5 achieved the best results, with a 28-day CS of 45.6 MPa, 9.9% higher than the control. At 15% replacement, FS decreased by 19% (ESP800) and 9% (ESP900), and CS decreased by 27.5% and 20%, respectively. UPV indicated denser matrices up to 10% replacement, with porosity increasing at 15%. Statistical analysis showed curing duration as the most influential positive factor, replacement ratio as the strongest negative effect, and calcination temperature as consistently beneficial. Multiple linear regression and ANOVA confirmed the statistical significance of these variables and demonstrated high predictive accuracy ($R^2 > 0.9$).

Keywords: Eggshell powder, Cement, Mortar, Compressive strength, Flexural strength

Öz

Bu çalışmada, gıda endüstrisinin kalsiyum karbonat ($CaCO_3$) açısından zengin bir yan ürünü olan atık yumurta kabuğu tozunun (ESP) çimento esaslı harçlara ikame edilmesi incelenmiştir. Yumurta kabukları öğütülmüş ve iki saat süreyle 800 °C ve 900 °C'de kalsine edilerek ESP800 ve ESP900 üretilmiştir. ESP, çimentonun %5, %10 ve %15'i oranında ikame edilerek yedi farklı harç karışımı hazırlanmıştır. Termal ve mikroyapısal özellikler TG/DSC, FE-SEM ve XRD ile analiz edilmiştir. İşlenebilirlik, yayılma tablası deneyi ile değerlendirilmiş; 7 ve 28 gün kür edilen numuneler üzerinde ultrases geçiş hızı (UPV), eğilme dayanımı (FS) ve basınç dayanımı (CS) testleri yapılmıştır. Kalsinasyon sıcaklığı ve ikame oranı, performansı önemli ölçüde etkilemiştir. %5 ikamede, ESP900-5 karışımı 28 günlük CS değerinde 45.6 MPa'ya ulaşarak kontrole kıyasla %9.9'luk bir artış sağlamıştır. %15 ikamede ise FS değerleri ESP800'de %19, ESP900'de %9; CS değerleri ise sırasıyla %27.5 ve %20 azalmıştır. UPV sonuçları, %10'a kadar ikame seviyelerinde daha yoğun matrisler oluştuğunu, %15 ikamede ise gözenekliliğin arttığını göstermiştir. İstatistiksel analizler, kür süresinin FS ve CS üzerinde en etkili olumlu faktör, ikame oranının en güçlü olumsuz etken ve kalsinasyon sıcaklığının ise her iki dayanım parametresine de sürekli olarak olumlu katkı sağladığını ortaya koymuştur. Çoklu doğrusal regresyon ve ANOVA analizleri, bu değişkenlerin istatistiksel olarak anlamlı olduğunu doğrulamış ve yüksek tahmin doğruluğu ($R^2 > 0.9$) göstermiştir.

Anahtar kelimeler: Yumurta kabuğu tozu, Çimento, Harç, Basınç dayanımı, Eğilme dayanımı

1 Introduction

The cement production process is highly energy-intensive and releases substantial amounts of carbon dioxide into the atmosphere. Similarly, the extraction of natural aggregates requires considerable energy and contributes to increased greenhouse gas emissions. Combined with the widespread use of cement-based construction materials, this leads to the rapid depletion of natural resources and significant environmental degradation [1]. Cementitious composites are the second most consumed material in the world after water and are extensively used in the construction sector [2].

In recent years, research on the utilization of industrial waste as a partial replacement for cement or aggregates has gained momentum [3, 4]. In addition to industrial by-products, biological and agricultural wastes have gained interest as supplementary cementitious materials owing to their renewability and widespread availability [5]. In this context, eggshells—generated in large quantities through the poultry industry and widely consumed in the agricultural and

food sectors—stand out among eco-friendly biological wastes because of their easy accessibility and low cost [6].

Given the environmental burden associated with conventional Portland cement production—which involves extraction, grinding, and sintering of raw materials at temperatures exceeding 1400 °C—there is a growing interest in alternative binders that require lower thermal energy. In this regard, the calcination of eggshell waste to produce eggshell powder (ESP) is typically performed at 800–900 °C for about 1–2 hours, far below the clinkerization temperature of cement manufacturing. Consequently, ESP preparation consumes less energy and emits substantially lower CO_2, providing a more sustainable and low-carbon alternative for partial cement replacement in concrete [7,8].

Similar evidence of calcination-induced activation has been reported for other mineral additives. In a study on high-strength mortars, Sarıdemir et al. [9] showed that replacing cement with calcined diatomite powder (5–20%) significantly enhanced pozzolanic reactivity when calcined at 850 °C and improved both mechanical strength and residual performance after exposure to 400–1000 °C. Moreover, Ruan et al. [10] found that incorporating calcined clay and limestone powder at 50–70% cement replacement did not result in a substantial increase in compressive strength but contributed to microstructural densification, improved toughness, and refined pore structure in cementitious materials. These findings collectively indicate that calcination at moderate-to-high temperatures (≈800–900 °C) can substantially activate various siliceous and calcareous materials, enhancing their reactivity and performance in blended systems.

Eggshell waste can be collected from households, restaurants, bakeries, catering services, and poultry farms [11]. However, improper management of such waste poses risks to public health and may lead to environmental problems [12]. Despite generating 8–10 million tons of waste annually worldwide, the industrial utilization rate of eggshell by-products remains below 5%, causing landfill burdens and disposal-related environmental concerns; therefore, valorizing eggshells as a calcium-rich cementitious resource offers significant practical and industrial relevance [13]. Moreover, the circular utilization of ESP contributes to resource efficiency in the cement industry, as its $CaCO_3$-rich composition enables partial substitution of limestone powder in blended cements, supporting decarbonization efforts [14]. Beyond construction applications, eggshell waste has also demonstrated value in sectors such as environmental remediation, bioceramics, catalysis, and chemical production, further emphasizing its high resource potential [15].

Previous studies have compared untreated and calcined forms of eggshell powder. Jaber et al. [16] showed that while untreated ESP provided only minor strength gains, thermally treated ESP (750 °C) achieved markedly better performance, increasing compressive strength by 29 % and reducing water absorption by 30 % at 15 wt % replacement. This improvement was attributed to the conversion of $CaCO_3$ to reactive CaO during calcination, which enhances C–S–H formation and microstructural densification.

The primary constituent of eggshells is calcium carbonate ($CaCO_3$), which, when calcined at temperatures above 700 °C, decomposes to form calcium oxide (CaO) with basic characteristics [17]. Calcined ESP can accelerate hydration, promote C–S–H gel formation, and enhance mechanical performance, including long-term strength and chemical resistance [18]. This transformation enables partial self-cementing behavior and enhances the capability of calcined ESP to contribute CaO for hydration-driven gel formation in cementitious systems, rather than functioning as a conventional pozzolanic material. Accordingly, various researchers have investigated the effects of eggshell powder (ESP) and calcined eggshell powder (CESP) on cementitious mortars and concretes under different parameters.

Zhou et al. [19] mechanically cleaned eggshells collected as industrial waste, followed by calcination at 900 °C for three hours to remove organic matter and convert $CaCO_3$ to CaO. Using the ground powders, they produced silica-bonded, monetite-based cement, and reported that the addition of nanosilica increased the compressive strength from 8.5 MPa to 20.2 MPa. Wang et al. [13] calcined ESP at 900 °C for different durations (10, 20, and 30 minutes) to develop cementitious systems containing limestone; the inclusion of CESP increased the 28-day compressive strength by 32.3% and reduced the degree of carbonation by 33.4%. Similarly, Maglad et al. [20] utilized eggshell powder calcined at 900 °C for 120 minutes in the production of lightweight foamed concrete at replacement levels of 5–20%, identifying 15% as the optimum dosage. Maqsood and Eddie [21] investigated the influence of eggshells calcined at various temperatures and durations on setting time and hydration, revealing that the presence of $Ca(OH)_2$ played a decisive role in determining the setting behavior.

Khan et al. [2] examined the influence of ESP on water absorption capacity and reported that lower replacement levels reduced water uptake. Jaber et al. [16] found that processed ESP improved the properties of cement mortar to a greater extent than unprocessed ESP, whereas Grzeszczyk et al. [22] indicated that incorporating 10% ESP extended the setting time without adversely affecting strength. Wei et al. [23] reported that fine ESP particles, with sizes smaller than cement particles, enhanced workability and improved mechanical strength at replacement levels of up to 5%.

These findings indicate that ESP and its calcined forms at different temperatures can have significant effects on the workability and mechanical performance of cement-based mortars. However, in the existing literature, studies that systematically evaluate the combined influence of calcination temperature and replacement ratio on both fresh mixture properties and hardened characteristics—such as ultrasonic pulse velocity, flexural strength, and compressive strength—are limited. In this study, eggshells sourced from the food and bakery industries were calcined at 800 °C and 900 °C, and incorporated into cement-based mortars at replacement levels of 5%, 10%, and 15%. Thermal behavior, microstructure, and particle size distribution were analyzed to evaluate the influence of calcination on the material characteristics, whereas performance changes were quantitatively examined through flow table measurements,

ultrasonic pulse velocity testing, and flexural and compressive strength evaluations. The novelty of this work lies in its comparative evaluation of the influence of ESP obtained at different calcination temperatures on both fresh and mechanical properties, supported by experimental and statistical analyses. The results provide original insights for the optimal utilization of waste-derived calcium sources in sustainable binder design.

2 Materials and methods

2.1 Materials

Discarded chicken eggshells were sourced from nearby food establishments, including restaurants, bakeries, and cafés. They were thoroughly washed with tap water to remove adhering organic residues, ensuring material purity and preventing undesirable reactions during subsequent processing. The cleaned shells were oven-dried at 70 °C for approximately 24 hours to remove remaining moisture and then manually pre-crushed. The crushed material was ground in a laboratory-scale ball mill operating at 60 rpm for 2 hours, resulting in a particle size distribution in which 90% of the particles were below 75 µm. The ground powder was sieved through a 75 µm mesh, and the undersized fraction—having a specific gravity of 2.48 g/cm³—was designated as eggshell powder (ESP) for use in the study (Figure 1).

Figure 1. Preparation of eggshell powder

In the literature, calcination of eggshell powder (ESP) at temperatures between 700 °C and 900 °C for 1–3 hours has been reported to effectively remove organic compounds and impurities [1, 2, 17]. In this study, the prepared ESP samples were calcined in an electric furnace at a heating rate of 10 °C/min to target temperatures of 800 °C and 900 °C, with each temperature maintained for 2 hours (Figure 2). Following calcination, the samples were allowed to cool naturally to ambient temperature (20 °C) over a 24-hour period. The resulting calcined products were designated according to calcination temperature: ESP800 (specific gravity: 2.39 g/cm³) for the material calcined at 800 °C and ESP900 (specific gravity: 2.31 g/cm³) for the material calcined at 900 °C.
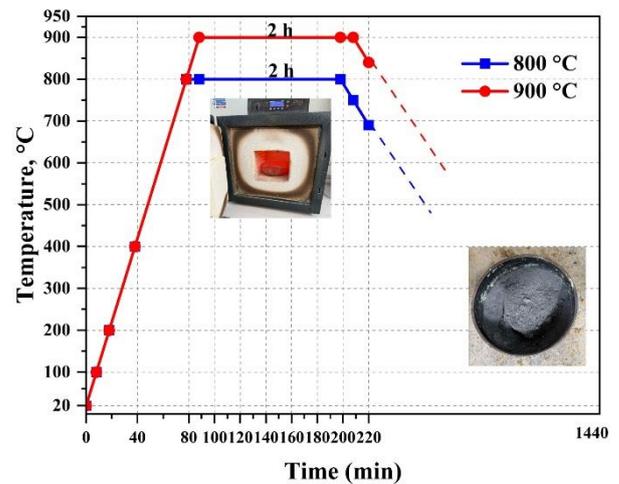

Figure 2. Calcination of ESP in an electric furnace at different temperatures for 2 hours

Using a NETZSCH STA 449 thermal analyzer, thermogravimetric (TG) and differential scanning calorimetry (DSC) analyses were conducted to assess mass loss, thermal decomposition behavior, and characteristic properties of ESP800 and ESP900 over the temperature range of 25–900 °C. The tests were designed to quantitatively assess the thermal stability of the samples and the transformations occurring during calcination. Each specimen was heated from room temperature to 900 °C in a nitrogen environment at a controlled heating rate of 10 °C/min, with the TG/DSC outcomes displayed in Figure 3. The TG curve shows negligible mass change between 25–100 °C, indicating low hygroscopicity and minimal initial moisture content. Between 100–600 °C, a slight mass loss is observed, attributed to the removal of bound water and partial decomposition of organic residues. Beyond this range, the primary decomposition process begins, with a pronounced slope appearing around 700 °C and continuing up to 850–900 °C. In this interval, mass decreased by approximately 47%, stabilizing at around 52.96% of the initial value. This significant loss corresponds to the decomposition of calcium carbonate ($CaCO_3 \rightarrow CaO + CO_2$), where CO_2 release is the main cause of the reduction. The DSC curve supports these findings, displaying a distinct endothermic peak near 800 °C, characteristic of $CaCO_3$ decomposition. At lower temperatures, energy changes were minimal, with no notable endothermic or exothermic events. Overall, the results confirm that ESP is thermally stable at lower temperatures, with major structural changes occurring between 800–900 °C, and that it predominantly consists of calcium carbonate, consistent with previous studies [5, 22, 24].

In the production of mortar series, CEM I 42.5R Portland cement (specific gravity: 3.1 g/cm³) supplied by Vezirhan Cement Plant was used. The chemical compositions of ESP, ESP800, ESP900, and cement were determined using X-ray fluorescence (XRF) analysis, and the results are presented in Table 1. In addition, the microstructures of these materials were examined using field emission scanning electron microscopy (FE-SEM) and are shown in Figure 4
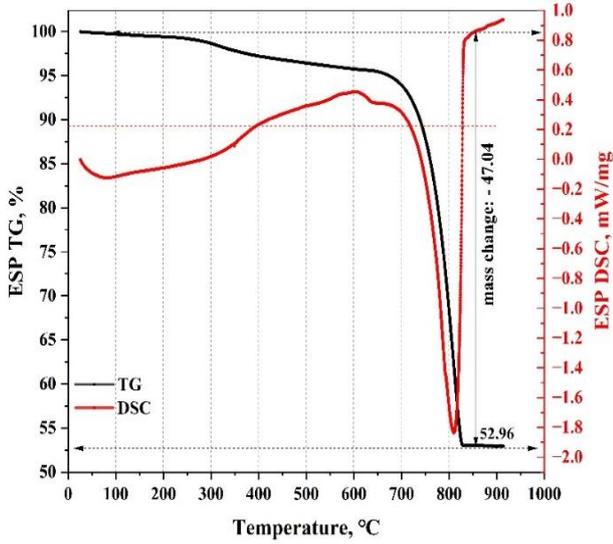
Figure 3. TG and DSC analyses of ESP

Table 1. Chemical compositions of the powdered materials

Oxide Components, %	ESP	ESP 800	ESP 900	CEM I 42.5R
SiO_2	0.1	0.1	0.1	18.7
Al_2O_3	0.1	0.1	0.1	4.6
Fe_2O_3	0.2	0.1	0.3	3.4
CaO	60.6	67.4	76.6	63.7
MgO	0.62	0.68	0.82	1.3
SO_3	0.01	0.05	0.02	2.7
K_2O	0.02	0.03	0.05	0.7
TiO_2	0.01	0.01	0.01	-
P_2O_5	0.01	0.01	0.01	-
Mn_2O_3	0.01	0.01	0.02	-
Loss of ignition	36.9	31.2	21.1	3.9

(Chemical properties (XRF))

The FE-SEM micrograph of the CEM sample (Figure 4a) shows that cement particles generally possess an angular, multifaceted morphology with fractured edges. In contrast, the ESP micrograph (Figure 4b) reveals noticeably larger particles with irregular, planar shapes. Particle diameters ranging from 46.2 to 55.1 µm indicate the natural and porous structure of the material prior to calcination. The ESP800 sample (Figure 4c), produced after thermal treatment at 800 °C, exhibits more compact, angular, and fragmented particles, with sizes generally below 17.8 µm. This confirms that calcination causes a distinct transformation in both particle size and morphology.

The ESP900 sample (Figure 4d) shows even greater particle size reduction under higher calcination temperature, producing sharper-edged, denser particles, with most diameters below 12.8 µm. Furthermore, the irregular and heterogeneous crystalline structure observed in uncalcined ESP becomes more uniformly distributed after 2 hours of calcination at 900 °C, with a well-developed porous morphology emerging on particle surfaces [17]. The increase in calcination temperature accelerates carbonate decomposition, leading to finer particle sizes, higher surface density, and improved microstructural integrity. These changes are considered advantageous, as they may enhance its effectiveness as a micro-filler and CaO-rich reactive additive that promotes hydration and secondary gel formation, rather than acting as a traditional pozzolanic source.
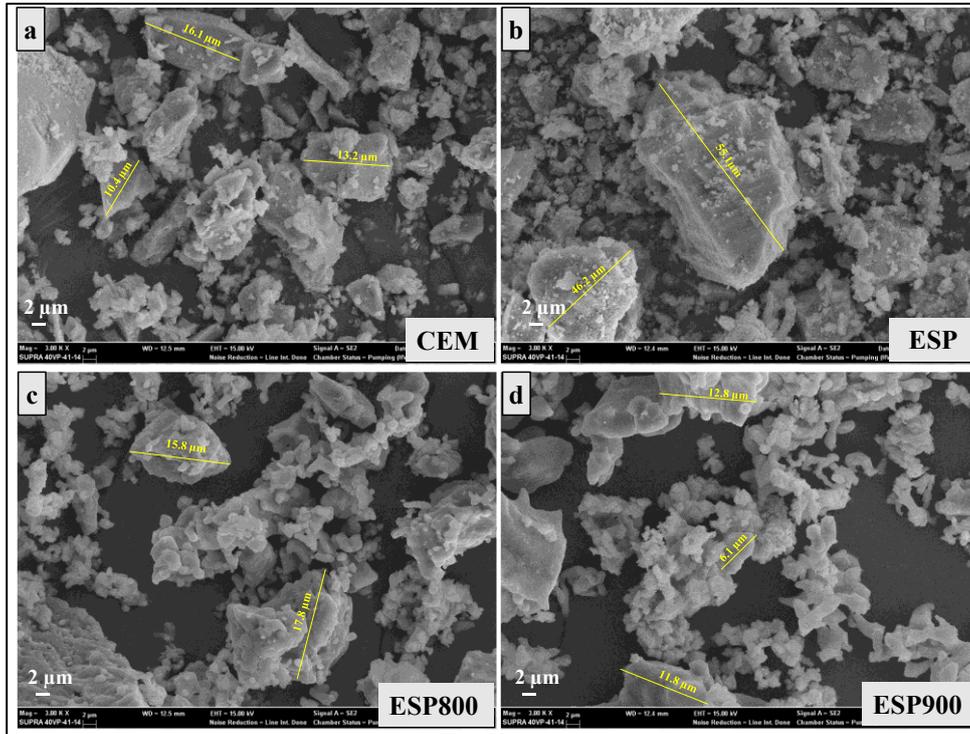

Figure 4. FE-SEM images of the powdered materials at 3000× magnification: (a) CEM, (b) ESP, (c) ESP800, (d) ESP900

The X-ray diffraction (XRD) patterns of ESP, ESP800, and ESP900, recorded within the 2θ range of 10°–80°, are shown in Figure 5. All samples exhibited characteristic calcite ($CaCO_3$) peaks, denoted by the letter "C," with the most intense reflection consistently observed at approximately 2θ = 29.5°. Several additional well-defined peaks within the 23°–52° 2θ range further confirmed the crystalline structure of calcite in each sample. Peak intensities decreased with increasing calcination temperature, measured as 11.777 A.U. for ESP, 11.132 A.U. for ESP800, and 6.637 A.U. for ESP900. The marked reduction of up to 40% in ESP900 relative to ESP800 suggests not only the onset of thermal decomposition at 900 °C but also microstructural changes such as internal cracking or the development of porosity. No new diffraction peaks attributable to calcium oxide (CaO) were detected, indicating either incomplete decomposition or the presence of CaO in an amorphous phase undetectable by XRD.
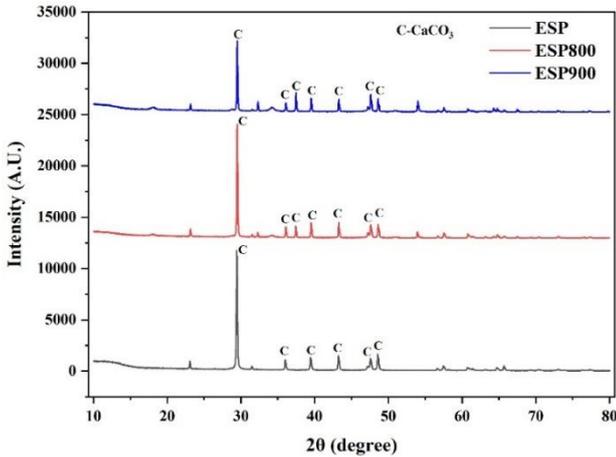

Figure 5. XRD patterns of ESP, ESP800 and ESP900

These results are consistent with previous studies [5, 25] on the thermal behavior of eggshell-derived, calcium carbonate-based materials.

River sand (fineness modulus: 2.55) sourced from the Osmaneli region was used as the aggregate in the production of the mortar series. The sand exhibited a particle size distribution of 0–4 mm, a specific gravity of 2.61 g/cm³, and a water absorption capacity of 1%. Particle size distributions for ESP800, ESP900, cement, and river sand were determined using a Mastersizer 2000 analyzer, and the results are shown in Figure 6. As illustrated, ESP900 exhibited a finer and narrower particle size distribution than ESP800, attributed to the effect of high-temperature calcination. For ESP900, 90% of the particles (d90) were smaller than 52.4 μm, whereas for ESP800 this value was 60.2 μm. The median particle sizes (d50) were measured as 7.9 μm for ESP900 and 13 μm for ESP800. Municipal tap water was used as the mixing water in the preparation of the mortar series.
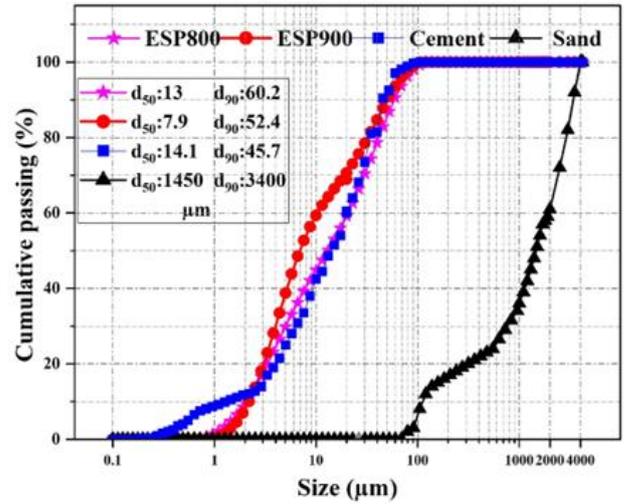

Figure 6. Particle size distribution curves of powders and sand

2.2 Methods

The mortar mixtures were prepared in seven series using a mechanical mixer in accordance with TS EN 196-1 [26]. ESP800 and ESP900 were incorporated as partial cement replacements at levels of 5%, 10%, and 15% by weight, while a control series (C) containing only cement as the binder was also produced. In all mixtures, the aggregate-to-binder ratio was fixed at 3 and the water-to-binder ratio at 0.5, with no superplasticizers or other chemical admixtures used. In this study, the term "binder" refers to the combination of cement and the specified proportion of ESP800 or ESP900. The series were designated as C, ESP8-5, ESP8-10, ESP8-15, ESP9-5, ESP9-10, and ESP9-15, where "ESP8" denotes ESP calcined at 800 °C and "ESP9" denotes ESP calcined at 900 °C, with the numerical suffix indicating the percentage by weight of cement replaced. For example, ESP8-5 refers to a mixture in which 5% of the binder consists of ESP calcined at 800 °C. Table 2 presents the material compositions and mix proportions for all mortar series.

The mixing procedure strictly followed TS EN 196-1. [26]. (a) Water was first poured into the mixing bowl, followed by the addition of cement (or cement + ESP). (b) The mixer was immediately started at low speed, and after 30 s, river sand was gradually introduced within 30 s while mixing continued. The mixer was then switched to high speed and operated for an additional 30 s. (c) After a total mixing time of 1 min 30 s, the mixer was stopped, and any mortar adhering to the sides and bottom of the bowl was scraped toward the center using a rubber scraper for 15 s. (d) Finally, the mixer was restarted at high speed for another 60 s.

The workability of the fresh mortar mixtures was evaluated using the flow table method in compliance with TS EN 1015-3/A2 [27]. For each series, six prismatic specimens with dimensions of 40 mm × 40 mm × 160 mm were prepared. The fresh mortar was placed into the molds in two layers, with each layer compacted using a jolting apparatus.

The specimen surfaces were then covered with plastic sheets and stored in the laboratory environment (20 ± 2 °C) for 24 hours. After demolding, the hardened mortar specimens were immersed in lime-saturated water (20 ± 2 °C) until the completion of the 7- and 28-day curing periods, after which they were subjected to hardened mortar tests. The tests performed included: ultrasonic pulse velocity (UPV) measurement in accordance with TS EN 12504-4 [28], flexural strength testing in accordance with TS EN 1015-11 [29], and compressive strength testing conducted on the two halves obtained from each flexural test specimen.

Table 2. Mix proportions and mortar series

Series	CEM (g)	ESP800 (g)	ESP900 (g)	Sand (g)	Water (mL)
C	450	-	-	1350	225
ESP8-5	427.5	22.5	-	1350	225
ESP8-10	405	45.0	-	1350	225
ESP8-15	382.5	67.5	-	1350	225
ESP9-5	427.5	-	22.5	1350	225
ESP9-10	405	-	45.0	1350	225
ESP9-15	382.5	-	67.5	1350	225

Flexural strength testing was performed at a loading rate of 0.05 kN/s, whereas compressive strength testing was conducted at an increased rate of 2.4 kN/s. UPV measurements were performed using a UTC-3034 microprocessor-controlled device, capable of measuring transit times in the range of 0.1–1999.9 µs with a resolution of 0.1 µs. All test results were reported as the average of values obtained from at least three specimens for each series.

3 Result and discussion

3.1 Flowability

Flow table test measurements of the mortar mixtures' spread diameters are illustrated in Figure 7. As shown, the values ranged from 135 mm to 150 mm. The maximum flow diameter of 150 mm was observed in the ESP8-5 mixture, in which 5% of the cement was replaced with ESP800. In contrast, the lowest value, 135 mm, was observed in the ESP9-15 series with a 15% replacement using ESP900. The control series (C) exhibited a flow diameter of 145 mm.

Among the ESP800-incorporated mixtures, only the ESP8-5 series with a 5% replacement level exhibited improved workability, showing a 3.4% increase in flow diameter compared to the control series. At a 10% replacement (ESP8-10), the flow diameter matched that of the control, whereas at 15% replacement (ESP8-15), it decreased to 140 mm, corresponding to a 3.4% reduction. For the ESP900-incorporated mixtures, a 5% replacement (ESP9-5) resulted in a slight 1.4% increase over the control, but higher replacement levels led to a general decline in workability, with reductions of 3.4% for ESP9-10 and 6.9%

for ESP9-15. These results indicate that the effect of ESP on workability is influenced by both calcination temperature and replacement level. Calcination reduced particle size (Figure 6), produced sharper and more angular morphologies, decreased specific gravity, and increased microporosity—particularly in ESP900. Such microstructural changes directly affected water distribution, inter-particle friction, surface area, and packing density in fresh mortars.
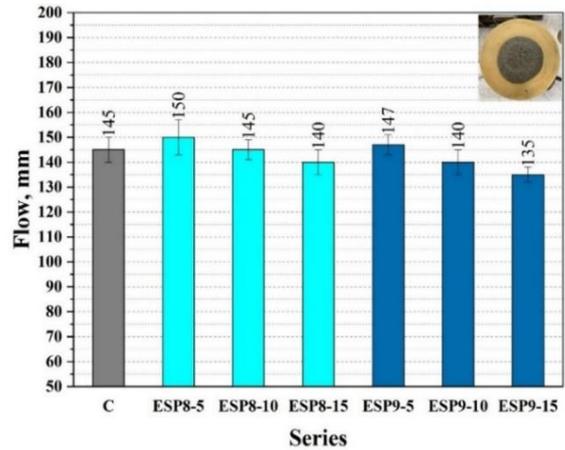
Figure 7. Flow diameters of mortar series under testing

The improvement in workability observed in the ESP8-5 and ESP9-5 series can be attributed to the low replacement level, which promotes the formation of an effective interfacial transition zone with cement, allows the porous structure to facilitate dispersion without excessive water absorption, and benefits from the lower density of ESP compared to cement. Additionally, the smaller particle sizes of ESP800 and ESP900 relative to cement (Figure 6) enable these particles to fill voids between cement grains, thereby releasing entrapped mixing water and reducing inter-particle friction—an effect that enhances mortar flowability [4]. Conversely, at higher replacement levels (≥10%), the increased surface area of the finer ESP particles, as evidenced by the FE-SEM observations in Figure 4 (c–d) and the particle size distributions shown in Figure 6, leads to greater water adsorption and higher inter-particle friction, resulting in reduced flow diameters. Similar reductions in flowability at elevated ESP contents have been reported in previous studies, which attributed the decline to increased water absorption and the lower specific gravity of ESP compared with cement [18, 20]. In particular, the smaller and denser structure of ESP900, combined with its lower specific gravity, causes it to occupy a greater volume within the mix, increasing water demand and making it the series with the most pronounced reduction in workability.

3.2 Ultrasonic pulse velocity test results

According to the ultrasonic pulse velocity (UPV) test results, higher UPV values indicate that the mortar matrix possesses a more homogeneous, dense, and high-quality structure, whereas lower UPV values suggest the presence of cracks, voids, or other discontinuities within the internal

structure [30]. Therefore, UPV measurements serve as an important non-destructive indicator for assessing the internal structural integrity of the specimens and identifying potential defects.

Figure 8 shows the average UPV values of the mortar mixtures after 7 and 28 days of curing. As seen in the figure, notable variations in UPV values are observed depending on the curing period and the replacement ratio.

The control mixture exhibited a 7-day UPV value of 4010 m/s. For the ESP800 series, UPV values ranged from 3700 to 4095 m/s, whereas for the ESP900 series, they ranged from 3850 to 4280 m/s. A comparison between the two series shows that, particularly at the 5% replacement level, ESP900 achieved higher UPV values. At this level, both ESP8-5 and ESP9-5 exhibited increases relative to the control mix, with gains of approximately 2.1% and 6.7%, respectively. This improvement can be attributed to the finer and more reactive particles of ESP900, calcined at 900 °C, which enhance matrix density. At the 10% replacement level, the ESP9-10 series recorded a UPV value about 5.7% higher than its ESP800 counterpart. At the highest replacement level (15%), ESP900 showed a UPV approximately 4.1% greater than ESP800; however, both series presented lower UPV values than the control. These findings indicate that increasing the replacement level promotes higher porosity in the mixture, which in turn reduces ultrasonic pulse velocity.

At 28 days, the UPV value for the control series was 4280 m/s. The ESP800 series exhibited values between 3800 and 4350 m/s, whereas the ESP900 series ranged from 4100 to 4500 m/s. The highest value, 4500 m/s, was achieved by the ESP9-5 series, corresponding to an increase of approximately 5.1% compared to the control. UPV values between 3600 and 4500 m/s are typically classified as 'good' concrete quality, while values exceeding 4500 m/s indicate 'excellent' matrix density and durability in cementitious composites [5, 31, 32]. This improvement is attributed to the high calcium oxide content of ESP900, which, when combined with the silica-rich composition of the cement mortar, enhances matrix density and contributes positively to structural integrity [30]. At the highest replacement level (15%), both series recorded lower UPV values than the control, with ESP8-15 measuring 3800 m/s (11.2% reduction) and ESP9-15 showing a 4.2% reduction. Notably, the UPV of ESP9-15 was about 7.9% higher than that of ESP8-15, indicating that while low ESP contents can improve matrix density and performance, higher contents tend to increase porosity, thereby reducing UPV.

3.3 Flexural strength test results

Figure 9 presents the flexural strength results of the mortar mixtures after 7 and 28 days of curing. At 7 days, the ESP8-5, ESP8-10, and ESP8-15 series recorded decreases of approximately 1%, 7%, and 10%, respectively, compared to the control series. In contrast, the ESP9-5 series exhibited a 4% increase, while the ESP9-10 and ESP9-15 series showed reductions of 2% and 7%, respectively. These results indicate that, at early ages, only the ESP9-5 mixture enhanced flexural strength, whereas all other replacement levels led to lower values than the control.
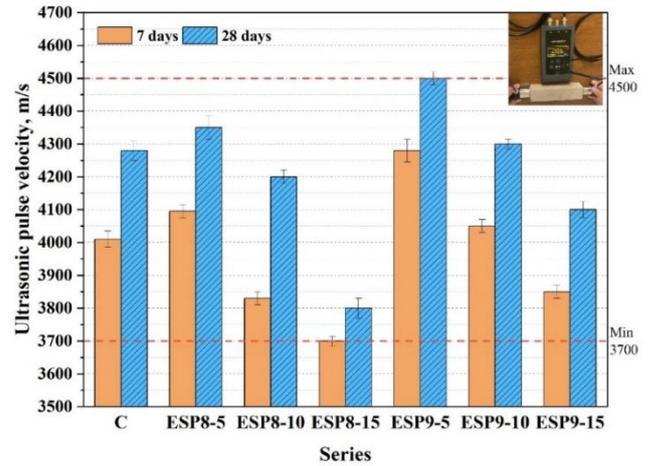
Figure 8. UPV measurements of the mixtures after 7 and 28 days of curing
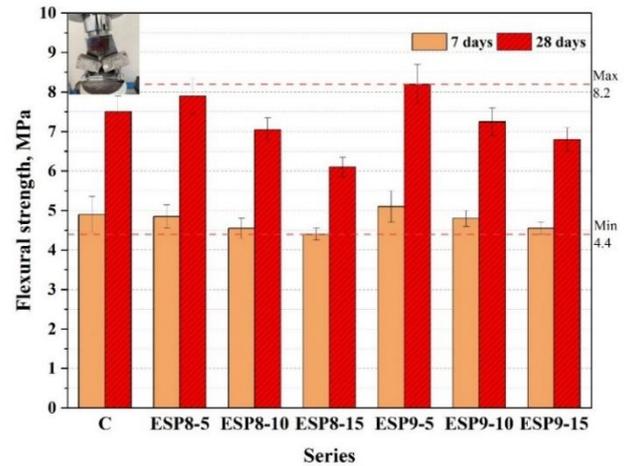
Figure 9. Flexural strength values of the series after 7 and 28 days of curing

At 28 days, the ESP8-5 and ESP9-5 series exhibited flexural strength increases of approximately 5% and 9%, respectively, compared to the control series. In contrast, ESP8-10 and ESP8-15 showed reductions of 6% and 19%, while ESP9-10 and ESP9-15 decreased by 3% and 9%, respectively. These results indicate that low ESP replacement levels (5%) can enhance flexural strength by improving the interfacial transition zone (ITZ) within the matrix. This improvement is particularly evident for ESP900, whose finer particles can fill voids between cement grains, strengthening the ITZ between cement paste and sand. At higher replacement levels, however, disruption of microstructural continuity reduces strength. Comparable trends were reported Maglad et. al., (2024) [20], who investigated calcined eggshell powder (CESP) in lightweight foamed concrete and observed that increasing CESP content enhanced both flexural and compressive strengths up to an optimum level (15 %), beyond which performance declined. Their SEM analyses attributed the improvement to densified microstructure and refined pore dispersion.

This behavior is also consistent with [23], who found that cement replacement with 2.5–10 % ESP resulted in maximum strength at 5 %, confirming the positive contribution of finely ground ESP to matrix densification. This behavior is consistent with previous studies reporting that low dosages of mineral additives improve strength through a pore-filling effect [23].

3.4 Compressive strength test results

The variation in compressive strength of the mortar series with curing time is presented in Figure 10. As shown, increasing the curing period enhanced the strength of all series. At 7 days, the compressive strength of the control (C) series was measured at 31.5 MPa. For the ESP800-incorporated series, the compressive strengths were 32.6 MPa for ESP8-5 and 28.5 MPa for ESP8-10, while ESP8-15 exhibited a further decrease to 23.6 MPa. In the ESP900-incorporated series, ESP9-5 reached 33.5 MPa—representing a 6.3% increase over the control—thereby demonstrating the highest performance among all mixtures. In contrast, ESP9-10 and ESP9-15 recorded lower strengths of 29.5 MPa and 24.8 MPa, respectively.

At 28 days, the control series reached 41.5 MPa. In the ESP800 series, ESP8-5 achieved 42.2 MPa (+1.7%), while ESP8-10 and ESP8-15 showed reductions to 36.4 MPa (−12.3%) and 30.1 MPa (−27.5%), respectively. In the ESP900 series, ESP9-5 attained the highest strength of all mixtures at 45.6 MPa (+9.9%), whereas ESP9-10 and ESP9-15 recorded 40.2 MPa (−3.1%) and 33.2 MPa (−20%), respectively.

A general evaluation indicates that low replacement levels (5%) in both the ESP800 and ESP900 series improved compressive strength at both early and later ages. This enhancement is attributed to the micro-filler effect of finely ground calcined ESP, which refines the pore structure and promotes the nucleation of hydration products. Similarly, Alsharari et al. [33] observed that mortars incorporating ESP calcined at 900 °C for 3 h achieved maximum compressive strength at a 5 % replacement level, while further increases led to performance deterioration due to dilution of the cementitious matrix. At medium and high replacement levels (10% and 15%), however, the reduction in cement content, insufficient formation of hydration products, and decreased binder paste volume led to significant strength losses. Notably, ESP900, calcined at 900 °C, achieved the highest performance at the 5% replacement level (ESP9-5), but this benefit diminished at higher replacement ratios. The observed decline is likely due to the reduced volume of cementitious phases, which adversely affects the material's density and microstructural continuity.

Incorporating ESP at replacement ratios of up to 10% in cementitious mortars can improve workability to some extent by increasing the water-to-cement ratio of the mixture (Figure 7). The reduction in cement content increases the water available per particle, thereby creating more favorable conditions for cement hydration and facilitating the nucleation of calcium silicate hydrate (C–S–H) phases.

Previous studies [21] have also reported that the high CaO content of ESP accelerates the hydration process,

resulting in denser hydration products and improved mechanical performance. However, at higher replacement levels, cement dilution and the associated increase in porosity become the primary factors contributing to strength loss. Furthermore, the particle size of ESP is a critical parameter; finer particles tend to enhance strength through a micro-filler effect, whereas coarser particles can adversely affect mechanical properties [34].
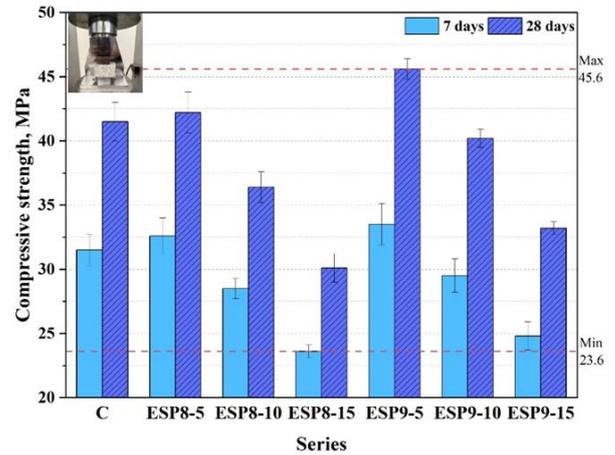

**Figure 10.** Compressive strength of the mixtures measured after 7- and 28-day curing periods

Finally, the findings revealed a direct and strong relationship ($R^2 > 0.8$) between UPV and compressive strength, as well as between flexural strength and compressive strength (Figure 11).

3.5 Statistical evaluations

In this study, multiple linear regression (MLR) and analysis of variance (ANOVA) methods were applied. MLR, as an extension of simple linear regression, models the relationship between a dependent variable and multiple independent variables [35]. The flexural strength (FS) and compressive strength (CS) results of the mortar series were used as dependent variables, while the calcination temperature of ESP (C, °C), ESP content (ESP, %), and curing duration (T, days) were considered independent variables. All statistical analyses were conducted in the Python programming environment at a 95% confidence level by evaluating the effects of independent variables on the dependent variables. Accordingly, the general form of the model derived from the MLR analysis is presented in Equation 1 [5].

$$Y = a_1x_1 + a_2x_2 + a_3x_3 + \dots\dots + a_nx_n + C \qquad (1)$$

As expressed in Equation 1, Y represents the model output, x_n denotes the independent input variables, and a_n refers to the partial regression coefficients. This model is widely employed to predict a dependent variable (strength) based on independent variables that exhibit a linear relationship [36].
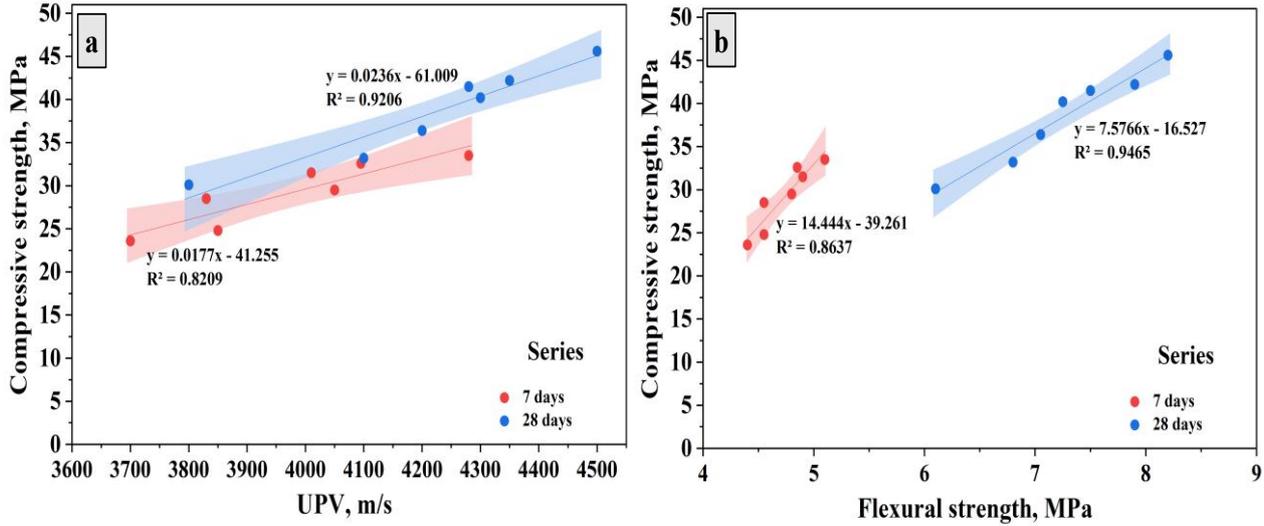
Figure 11. Relationships among compressive strength (CS), ultrasonic pulse velocity (UPV), and flexural strength (FS): (a) UPV vs. CS, (b) FS vs. CS

Within the scope of ANOVA, the relationships among the variables were evaluated using the F-statistic, p-value, and Durbin–Watson coefficient. A high F-statistic indicates that the independent variables have a significant effect on the dependent variable, while a p-value below 0.05 confirms the statistical significance of the model. The Durbin–Watson coefficient was used to assess the presence of autocorrelation. The effectiveness of multiple regression analysis (MRA) depends on the assumptions of linearity between independent and dependent variables and the independence of observations. High multicollinearity or strong correlations among independent variables can complicate the analysis. Values of the Durbin–Watson statistic between 1.5 and 2.5 are generally considered acceptable, indicating the absence of significant autocorrelation [37, 38]. In this study, the Durbin–Watson coefficients ranged between 1.74 and 2.41 (Table 3), confirming that the independence assumption was satisfied and validating the reliability of the regression model.

In the analyses, the calcination temperature was evaluated at three levels: 20 °C (representing the uncalcined state), 800 °C, and 900 °C. The dataset was randomly divided into two parts, with 80% used for training and 20% for testing, in order to assess the predictive accuracy of the models. Model performance was evaluated based on the coefficient of determination (R^2), mean absolute error (MAE), and root mean square error (RMSE). The coefficients of the obtained models are expressed in the following equations (Equations 2 and 3).

In the regression plots obtained through 5-fold cross-validation (Figure 12), the experimental values are presented on the x-axis, while the predicted values from the regression equations are shown on the y-axis. According to the analyses, both models demonstrated a high explanatory power ($R^2 > 0.9$), and the error values (MAE, RMSE) were found to be low. These findings confirm that the developed regression models can reliably predict the mechanical performance of mortars containing ESP under different calcination temperatures and curing conditions, consistent with the effectiveness of k-fold cross-validation methods [39] reported in the literatüre.

4 Conclusion

The evaluations presented below are based on the findings obtained from the experimental investigations;

- A 5% replacement with ESP800 increased flow by 3.4%, whereas 15% reduced it by the same amount. For ESP900, a 5% replacement improved flow by 1.4%, while 10% and 15% replacements led to decreases of 3.4% and 6.9%, respectively. The reduction at higher replacement levels is attributed to the fine particles produced at elevated calcination temperatures, which restrict water mobility.

- ESP incorporation up to 10% enhanced UPV, whereas 15% resulted in a reduction. In general, low-level ESP900 addition improved matrix density, thereby increasing UPV, while a 15% replacement at both calcination temperatures induced greater porosity, which adversely affected UPV.

- In terms of FS, a 4% improvement was observed only in the ESP9-5 series at 7 days, while all other series exhibited decreases. At 28 days, the ESP8-5 and ESP9-5 series achieved increases of 5% and 9%, respectively, compared to the control. However, 15% replacement in the ESP800 and ESP900 series resulted in reductions of 19% and 9%, respectively.

- Regarding CS, low replacement levels (5%) in both ESP800 and ESP900 series improved performance at both early (7 days) and later ages (28 days). At 28 days, increases of 1.7% for ESP8-5 and 9.9% for ESP9-5 were recorded. At higher replacement levels, however, reductions of up to 27.5% for ESP800 and 20% for ESP900 were observed in CS values.

Table 3. ANOVA results for the FS and CS of the mortar mixtures

Model		Sum of squares	df	Mean square	F	P- value	Durbin Watson value
FS (MPa)	ESP (%)	1.692	1	1.692	19.894	0.001	
	C (°C)	0.768	1	0.768	9.025	0.013	
	T (cure day)	22.252	1	22.252	261.574	<0.001	2.413
	Residual	0.851	10	0.085	-	-	
	Total	25.562	13	-	-	-	
CS (MPa)	ESP (%)	189.067	1	189.067	116.47	<0.001	
	C (°C)	60.353	1	60.353	37.18	<0.001	
	T (cure day)	303.646	1	303.646	187.05	<0.001	1.742
	Residual	16.234	10	1.623	-	-	
	Total	569.300	13	-	-	-	

$$FS = 4.1933 - 0.0936*(ESP) + 0.00075*(C) + 0.1159*(T) \qquad (2)$$

$$CS = 29 - 1.0114*(ESP) + 0.00807*(C) + 0.4294*(T) \qquad (3)$$
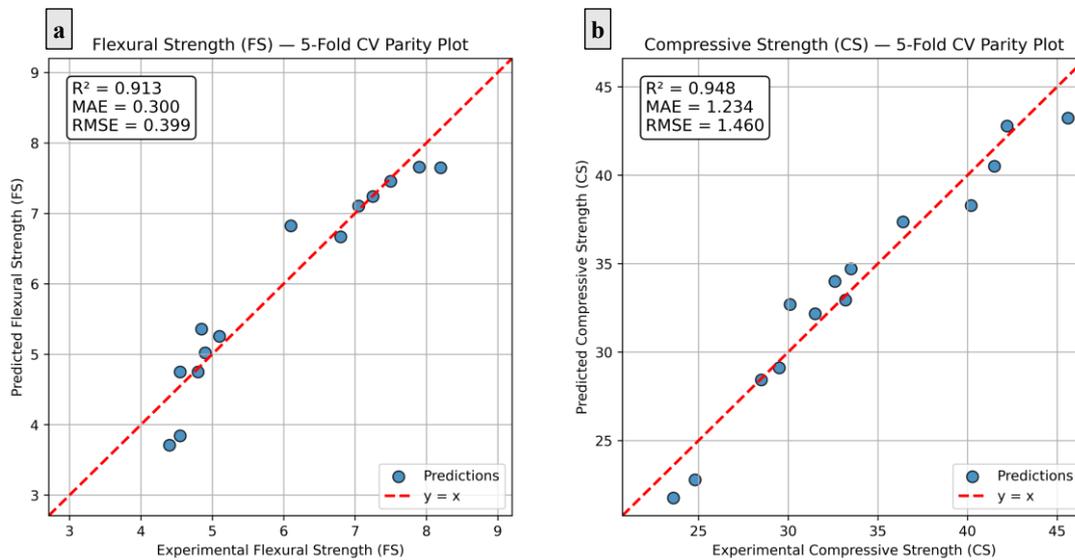
Figure 12. Scatter plots of experimental vs. predicted (a) FS and (b) CS with statistical metrics

- Statistical analyses revealed that curing time exerted the most significant positive effect on both FS and CS, whereas the ESP replacement ratio had the strongest negative effect. Calcination temperature exhibited a positive influence on both strength parameters, although its significance for FS was close to the threshold level.
- The optimum replacement level was determined as 5% ESP, which provided the most favorable balance between workability, density, and mechanical performance. At this level, the micro-filler effect and enhanced hydration kinetics led to improved compactness and strength. However, beyond this ratio, the combined effects of increased porosity and cement dilution became dominant, resulting in reduced strength and overall performance.
- In future studies, ESP could be incorporated into binder systems containing supplementary pozzolans, and its performance examined under different experimental conditions such as fiber addition or alternative curing methods.

Conflict of interest

The authors declare that they have no conflict of interest.

Similarity rate (iThenticate): %13

References

[1] D. Yang, J. Zhao, W. Ahmad, M. N. Amin, F. Aslam, K. Khan and A. Ahmad, Potential use of waste eggshells in cement-based materials: A bibliographic analysis and review of the material properties. Construction and Building Materials, 344, 128143, 2022.https://doi.org/10.1016/j.conbuildmat.2022.128143.

[2] K. Khan, W. Ahmad, M. N. Amin, and A. F. Deifalla, Investigating the feasibility of using waste eggshells in cement-based materials for sustainable construction. Journal of Materials Research and Technology, 23, 4059-4074, 2023. https://doi.org/10.1016/j.jmrt.2023.02.057.

[3] A. R. Boğa and A. F. Şenol, The effect of waste marble and basalt aggregates on the fresh and hardened properties of high strength self-compacting concrete. Construction and Building Materials, 363, 129715, 2023. https://doi.org/10.1016/j.conbuildmat.2022.129715.

[4] A. F. Şenol and C. Karakurt, Effect of Ground-Baked Clay and Marble Wastes on Strength Development of Cementitious Mortars. Journal of the Institute of Science and Technology, 13, 2692-2705, 2023. https://doi.org/10.21597/jist.1311857.

[5] A. F. Şenol and Ö. Çalışkan, Recycling bio-waste into durable green mortars: Effects of eggshell powder on strength, microstructure, and durability. Sustainable Chemistry and Pharmacy, 46, 102119, 2025. https://doi.org/10.1016/j.scp.2025.102119.

[6] A. H. Z. Chfat, H. Yaacob, N. H. M. Kamaruddin, Z. H. Al-Saffar and R. P. Jaya, Laboratory evaluation of micro and nano eggshell powder on physical and rheological properties of bitumen. Green Technologies and Sustainability, 3, 100212, 2025. https://doi.org/10.1016/j.grets.2025.100212.

[7] H.Y. Tiong, S. K. Lim, Y. L. Lee, C. F. Ong, and M. K. Yew, Environmental impact and quality assessment of using eggshell powder incorporated in lightweight foamed concrete. Construction and Building Materials, 244, 118341, 2020. https://doi.org/10.1016/j.conbuildmat.2020.118341.

[8] S. A. Salaudeen, S. M. Al-Salem, M. Heidari, B. Acharya, B., and A. Dutta, Eggshell as a carbon dioxide sorbent: kinetics of the calcination and carbonation reactions. Energy & Fuels, 33(5), 4474-4486, 2019. https://doi.org/10.1021/acs.energyfuels.9b00072

[9] M. Sarıdemir, S. Çelikten, and A. Yıldırım, Mechanical and microstructural properties of calcined diatomite powder modified high strength mortars at ambient and high temperatures. Advanced Powder Technology, 31(7), 3004-3017, 2020. https://doi.org/10.1016/j.apt.2020.05.024.

[10] Y. Ruan, T. Jamil, C. Hu, B. P. Gautam, and J. Yu, Microstructure and mechanical properties of sustainable cementitious materials with ultra-high substitution level of calcined clay and limestone powder. Construction and Building Materials, 314, 125416, 2022. https://doi.org/10.1016/j.conbuildmat.2021.125416.

[11] A. H. Z. Chfat, H. Yaacob, N. H. M. Kamaruddin, Z. H. Al-Saffar, and R. P. Jaya, Effects of nano eggshell powder as a sustainable bio-filler on the physical, rheological, and microstructure properties of bitumen. Results in Engineering, 22, 102061, 2024. https://doi.org/10.1016/j.rineng.2024.102061.

[12] M. S. Islam, and B. J. Mohr, Comparison of eggshell powder blended cementitious materials with ASTM Type IL cement-based materials. Cement, 17, 100109, 2024. https://doi.org/10.1016/j.cement.2024.100109.

[13] Y. S. Wang, R. Lin, T. Kim, J. Y. Lim, S. J. Kwon, and X. Y. Wang, Development and characterization of ternary blended cement incorporating slag and thermally activated waste eggshell: Hydration, microstructure, macro properties, and carbonation durability. Construction and Building Materials, 490, 142569, 2025. https://doi.org/10.1016/j.conbuildmat.2025.142569.

[14] B. W. Chong, P. Gujar, X. Shi, and P. Suraneni, Assessment of waste eggshell powder as a limestone alternative in portland cement. Materials and Structures, 57(10), 219, 2024. https://doi.org/10.1617/s11527-024-02478-9.

[15] T. Kalaycı, D. T. Altuğ, N. K. Kınaytürk, and B. Tunalı, Characterization and potential usage of selected eggshell species. Scientific Reports, 15(1), 6241, 2025. https://doi.org/10.1038/s41598-025-87786-y.

[16] H. A. Jaber, R. S. Mahdi and A. K. Hassan, Influence of eggshell powder on the Portland cement mortar properties. Materials Today: Proceedings, 20, 391-396, 2020. https://doi.org/10.1016/j.matpr.2019.09.153.

[17] L. M. Correia, R. M. A. Saboya, N. de Sousa Campelo, J. A. Cecilia, E. Rodríguez-Castellón, C. L. Cavalcante Jr, and R. S. Vieira, Characterization of calcium oxide catalysts from natural sources and their application in the transesterification of sunflower oil. Bioresource technology, 151, 207-213, 2014. https://doi.org/10.1016/j.biortech.2013.10.046.

[18] N. Hilal, T. K. M. Ali, A. S. Mohammed, A. S. Aadi, and Z. R. Harrat, Assessing the Durability of Eco-Friendly Mortars with Treated and Untreated Eggshell Powder as a Cement Substitute. International Journal of Civil Engineering, 1-17, 2025. https://doi.org/10.1007/s40999-025-01177-y.

[19] H. Zhou, T. J. Luchini, N. M. Boroujeni, A. K. Agarwal, V. K. Goel, and S. B. Bhaduri, Development of nanosilica bonded monetite cement from egg shells. Materials Science and Engineering: C, 50, 45-51, 2015. https://doi.org/10.1016/j.msec.2015.01.099.

[20] A. M. Maglad, M. A. O. Mydin, S. S. Majeed, B. A. Tayeh, and D. E. Tobbala, Exploring the influence of calcinated eggshell powder on lightweight foamed concrete: A comprehensive study on freshness, mechanical strength, thermal characteristics and transport properties. Journal of Building Engineering, 87, 108966, 2024. https://doi.org/10.1016/j.jobe.2024.108966.

[21] S. Maqsood and L. S. Eddie, Effect of using calcined eggshells as a cementitious material on early performance. Construction and Building Materials, 318, 126170, 2022. https://doi.org/10.1016/j.conbuildmat.2021.126170.

[22] S. Grzeszczyk, T. Kupka, A. Kalamarz, A. Sudot, K. Jurowski, N. Makieieva, K. Oleksowicz, R. Wrzalik, Characterization of eggshell as limestone replacement and its influence on properties of modified cement. Construction Building Materials, 319, 126006, 2022. https://doi.org/10.1016/j.conbuildmat.2021.126006.

[23] C. B. Wei, R. Othman, C. Y. Ying, R. P. Jaya, D. S. Ing and S. A. Mangi, Properties of mortar with fine eggshell powder as partial cement replacement.

Materials Today: Proceedings, 46, 1574-1581, 2021. https://doi.org/10.1016/j.matpr.2020.07.240.

[24] P. Intharapat, A. Kongnoo and K. Kateungngan, The Potential of Chicken Eggshell Waste as a Bio-filler Filled Epoxidized Natural Rubber (ENR) Composite and its Properties. Journal of Environmental Polymer Degradation, 21, 245–258, 2013. https://doi.org/10.1007/s10924-012-0475-9.

[25] M. Y. Xuan, R. S. Lin, T. B. Min and X. Y. Wang, Carbonation treatment of eggshell powder concrete for performance enhancement. Construction and Building Materials, 377, 130814, 2023. https://doi.org/10.1016/j.conbuildmat.2023.130814.

[26] Turkish Standards Institute. TS EN 196-1, 2016. Methods of testing cement – Part 1: Determination of strength. Ankara.

[27] Turkish Standards Institute. TS EN 1015-3, 2006. Methods of test for mortar for masonry- Part 3: Determination of consistence of fresh mortar (by flow table). Ankara.

[28] Turkish Standards Institute. TS EN 12504-4, 2021. Testing Concrete in Structures - Part 4: Determination of Ultrasonic Pulse Velocity. Ankara.

[29] Turkish Standards Institute. TS EN 1015-11, 2020. Methods of test for mortar for masonry - Part 11: Determination of flexural and compressive strength of hardened mortar. Ankara.

[30] N. N. A. Rasid, N. H. A. Khalid, A. Mohamed, A. R. M. Sam, Z. A. Majid and G. F. Huseien, Ground palm oil fuel ash and calcined eggshell powder as SiO2–CaO based accelerator in green concrete. Journal of Building Engineering, 65, 105617, 2023. https://doi.org/10.1016/j.jobe.2022.105617.

[31] B. Manjunath, C. M. Ouellet-Plamondon, B. B. Das, and C. Bhojaraju, Potential utilization of regional cashew nutshell ash wastes as a cementitious replacement on the performance and environmental impact of eco-friendly mortar. Journal of Building Engineering, 66, 105941, 2023. https://doi.org/10.1016/j.jobe.2023.105941.

[32] İ. Bekem Kara, Characterization of copper tailings in Murgul Copper Plant, Turkey, and its utilization potential in cement mortar with nano-and micro-silica.

Environmental Science and Pollution Research, 29(24), 36938-36950, 2022. https://doi.org/10.1007/s11356-021-18077-y.

[33] F. Alsharari, K. Khan, M. N. Amin, W. Ahmad, U. Khan, M. Mutnbak, M. Houda, and A. M. Yosri, Sustainable use of waste eggshells in cementitious materials: an experimental and modeling-based study, Case Studies Construction Materials, 17, e01620, 2022. https://doi.org/10.1016/j.cscm.2022.e01620.

[34] H. M. Hamada, B. A. Tayeh, A. Al-Attar, F. M. Yahaya, K. Muthusamy and A. M. Humada, The present state of the use of eggshell powder in concrete: A review. Journal of Building Engineering, 32, 101583, 2020. https://doi.org/10.1016/j.jobe.2020.101583.

[35] D.A. Emarah, Multivariate Predictive Modeling of Compressive Strength in Ground Granulated Blast Furnace Slag/Fly Ash-Based Alkali-Activated Concrete. Cleaner Engineering and Technology, 27, 101021, 2025. https://doi.org/10.1016/j.clet.2025.101021.

[36] M. A. M. Rihan, R. O. Onchiri, N. Gathimba, B. Sabuni and B. Pratap, Predicting Compressive Strength of Fly Ash and Sugarcane Bagasse Ash-Based Geopolymer Concrete Using Statistical Techniques. Journal of the Indian Chemical Society, 102, 101791, 2025. https://doi.org/10.1016/j.jics.2025.101791.

[37] S. Janga, A. N. Raut, M. Adamu, and Y. E. Ibrahim, Thermo-mechanical performance assessment of geopolymer synthesized with steel slag and glass owder at elevated temperatures. Powder Technology, 444, 120047, 2024. https://doi.org/10.1016/j.powtec.2024.120047.

[38] A. F. Şenol, Performance of geopolymer mortar incorporating spent coffee grounds as a recycled building material: An experimental and predictive analysis. Hybrid Advances, 10, 100479, 2025. https://doi.org/10.1016/j.hybadv.2025.100479.

[39] T. Fushiki, Estimation of prediction error by using K-fold cross-validation. Statistics and Computing, 21(2), 137-146, 2011. https://doi.org/10.1007/s11222-009-9153-8.